Известия Уральского государственного горного университета. 2018. Вып. 4(52). С. 7-17

Науки о Земле
Earth sciences

УДК 551.243(620)
https://doi.org/10.21440/2307-2091-2018-4-7-17

Structural evolution of Wadi Road El-Sayalla area, Eastern Desert, Egypt

Khaled Gamal ALI[1],
Hassan Ali ELIWA[2],
Masoud Salah MASOUD[1],
Mamoru MURATA[3],
Ahmed El Sayed ABDEL GAWAD[1,*]

[1]Nuclear Materials Authority, Cairo, Egypt
[2]Minoufiya University, Cairo, Egypt
[3]Naruto University of Education, National University Corporation, Naruto, Japan

Wadi Road El-Sayalla area is a part of the south Eastern Desert of Egypt. It comprises two plutons, Nikeiba basement rock complexes and Fileita Nubian sandstone. It is composed of metavolcanics, syenogranite, alkali feldspar granite and quartz syenite intruded by felsite and dolerite dikes and quartz veins at Nikeiba plutons which non-conformable overlain by Nubian sandstones at Fileita area.

Purpose of the work. The present work of this paper is to elucidate the interaction between inherited ductile fabrics and overprinting brittle structures. It is important to reconstruct the tectonic evolution of Wadi Road El-Sayalla area which help in constraining the mineralization trends in the study area.

Research methods. The folding related to ductile structures were analyzed using stereographic projection software packages GE Orient version 9.4.5. The fracture analyses related to brittle structures were carried out quantitatively using the paleostress analyses of the different sets to calculate the tensors related to the different compressional and extensional events using Tensor program.

Results. Structural evolution in the investigated area enabled the separation of five structural episodes: E1: syn-tectonic granite (tonalite-granodiorite); folding-thrusting episode associated with the cratonization of the arc/inter-arc rocks association. E2: Late-tectonic granite; upright folding episode associated with compression and shortening to the NE-SW direction. E3: Post-tectonic granite intrusion episode produced syenogranite and alkali feldspar granite of Nikeiba. E4 and E5: Early Cretaceous to Post Pleistocene episode is manifested by syncline folding along ENE-WSW detected in the Nubian sandstone of Fileita (E4). On the other hand, E5: Fracturing, faulting episode is characterized by multi-trends of fault populations (E-W strike slip (right; oldest), N-S strike slip (left), E-W dip slip, NE-SW strike slip (right) and NE-SW dip slip (youngest). Accessories as thorite, uranothorite, monazite, zircon, allanite, yttrocolombite and fluorite appear to be structurally controlled by the interaction between inherited ductile fabrics and overprinting brittle structures. The NE-SW, NW-SE, E-W, NNW-SSE and N-S normal faults are considered to be important deep seated structure trends which controlled many injections of felsite and dolerite dikes and alteration features that could have acted as good pathways for mineralization.

Keywords: Wadi Road El-Sayalla, Nikeiba, Fileita, Egypt, folding-thrusting, cratonization, folding episode, faulting episode.

Introduction

The studied area is a part of the basement complex in the Eastern Desert of Egypt; passed through several structural events since the early cratonization episode of the arc-inter-arc associations. So, the structural analyses of it enabled the separation of successive structural events including ductile and brittle deformations.

Many researchers have extensively studied structure evolution of the basement complexes and associated rocks in the Eastern desert of Egypt [1–7].

The structural field measurements were carried out on scattered pattern making use of the wadis in the area. They include primary structure measurements as bedding, secondary structures like foliation, deformed pebbles, faults, joints, minor and meso-scale folds. All the measurements were analyzed using different proper techniques "GE Orient version 9.4.5 and Tensor program according to [8–10]" to characterize the different structure that affected the area through out its geologic history.

Geologic setting

The exposed rock types at Wadi Road El-Sayalla are located between Latitudes 23°44'18"–23°54'36" N and longitudes 34°10'48"–34°24'36" E, in the Eastern Desert of Egypt (Fig. 1). Field studies indicate the presence of metavolcanics, tonalite-granodiorite, syenogranite, alkali feldspar granite and quartz syenite non-comfortably overlain by Nubian sandstone. Metavolcanics form a thick sequence of stratified lava flows interbanded with their pyroclastics. They are represented by ash and lithic lapilli metatuffs of basaltic, andesitic and dacitic composition. These rocks are intruded by tonalite-granodiorite, syenogranite, alkali feldspar granite and quartz syenite as well as by felsite dikes and quartz veins. Tonalite-granodiorite forms low relief masses and is non-comfortably overlain by Nubian sandstones at Fileita area. Tonalite-granodiorite consists of plagioclase, K-feldspar, quartz, hornblende and biotite. Syenogranite is low to moderate relief and is composed of K-feldspar, quartz, biotite, plagioclase and iron oxides. Alkali feldspar granite is the last phase at Nikeiba plutons. It is characterized by moderate relief and is composed of K-feldspar, plagioclase, quartz, and biotite. Quartz syenite forms high relief hills and is composed of K-feldspar, quartz, plagioclase, amphibole and biotite. Syenogranite and quartz syenite are highly albitized, hematitized and kaolinitized. Syenogranite, alkali feldspar granite and quartz syenite intrude the metavolcanics with well exposed intrusive contact. Felsite dikes cut the syenogranite, alkali feldspar granite and quartz syenite in the northeastern part of the mapped area. They are brecciated along the contact with metavolcanics and syenogranite. They are composed essentially of K-feldspar quartz and plagioclase together with subordinate biotite.

* gawadnma@gmail.com
http://orcid.org/0000-0002-2014-2677

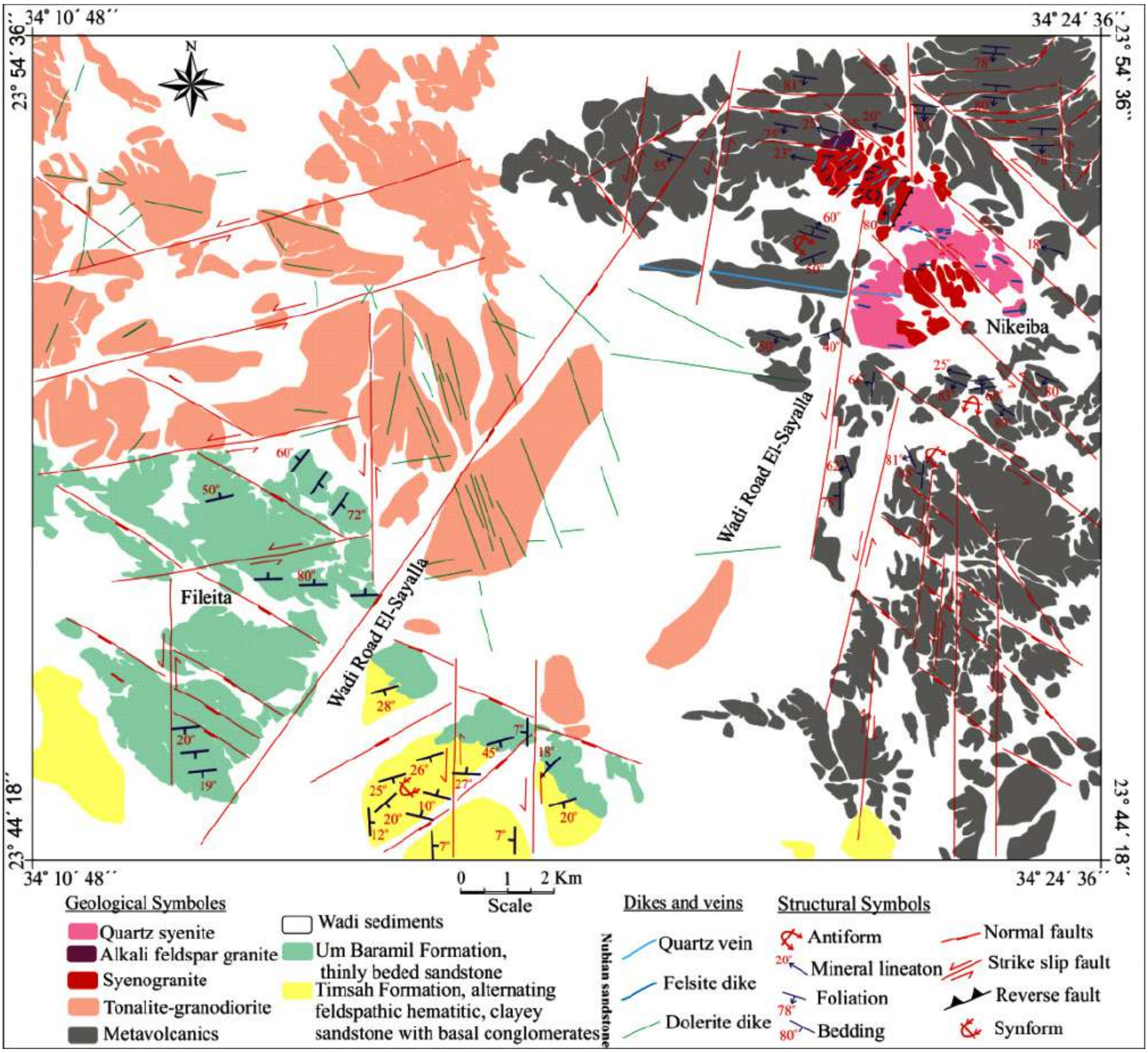

Figure 1. Geologic map of Wadi Road El-Sayalla area, Eastern Desert, Egypt.
Рисунок 1. Геологическая карта района Вади-роуд Эль-Саялла, Восточная пустыня (Египет).

Nubian sandstones include two Formations: lower Timsah Formation and upper Um Baramil Formation (Fig. 2). Timsah Formation attains 7.5 m thick, and comprises different types of cross-bedding, pebbly ferruginous, gradded bedding and clayey sandstones. Gradded- and cross-bedding features are observed as primary sedimentary structure in some sandstone beds. Um Baramil Formation is the most extensive exposure of Nubian sandstone in the investigated Fileita area. It overlies Timsah Formation and in other parts overlies the tonalite-granodiorite with non-conformity surface. This formation attains 70 m in thickness and comprises yellowish to dark grey sandstone, kaolinitic sandstone and pebbly ferruginous sandstone. Timsah and Um Baramil formations are traversed by N-S strike slip sinstral faults (Fig. 1).

Structural analyses

The studied area is an object of an intensive detailed systematic analysis of the structural fabrics (bedding, foliation, fold axes, fault populations, joints and liniments) collected from different sites distributed all the outcropping rock types (Fig. 1). During the detailed field study, the chronological criteria (cross-cut relationships, overprinting relations, overprinting of marks, reactivation geometries as well as fold-fault relationships) have been carefully documented in order to define the succession of the deformational events. A fundamental concept in structural analysis is the proposition that the small-scale structures in the field can act as a guide to the large-scale regional features that are not visible to the field observer.

Ductile fabrics

Field observations indicate that the ductile deformation was restricted only to highly sheared metavolcanics as regional isoclinal and upright folds with pervasive NW-SE and ENE-WSW foliations. Ductile deformation is studied by analyzing the measured structural elements represented by foliations and minor fold axes, using the lower hemisphere stereographic projection. Based on measurements of foliation, lineaments and fold axes have been collected from different sites distributed along the metavolcanics exposures. These measurements have been categorized and analyzed according to its trend distribution. Each system of foliation has been analyzed to deduce its principal compression direction as well as their corresponding inferred tectonic regime.

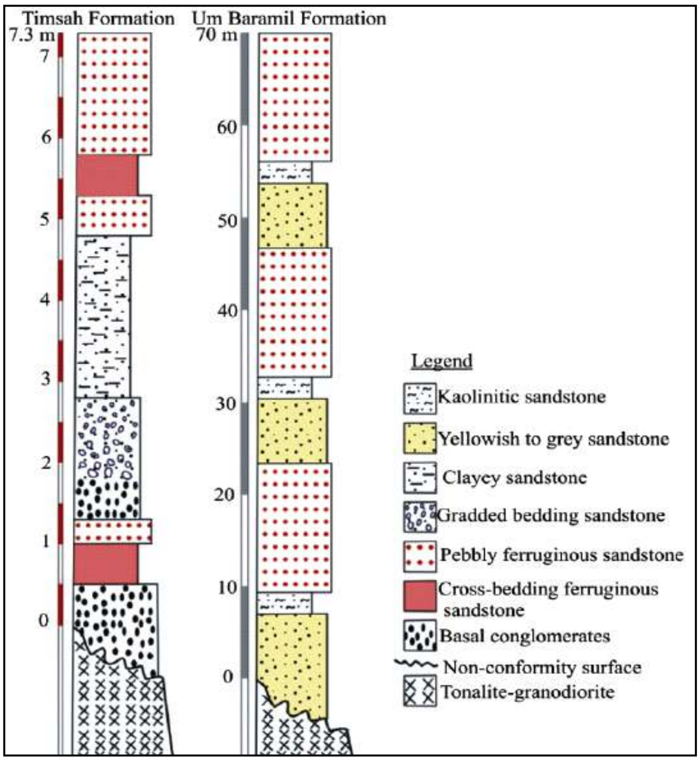

Figure 2. Schematic lithological profiles show the nonconformity surface between tonalite-granodiorite and Nubian sandstone successions in Timsah Formation (7.3 m) and Um Baramil Formation (70 m) at Wadi Road El-Sayalla (Fileita area), Eastern Desert, Egypt.
Рисунок 2. Схематические литологические профили показывают несогласие между тоналит-гранодиоритами и нубийскими песчаниками в Тимсахской свите (7,3 м) и Ум-Барамильской свите (70 м) на Вади-роуд Эль-Саялла (район Филейты), Восточная пустыня (Египет).

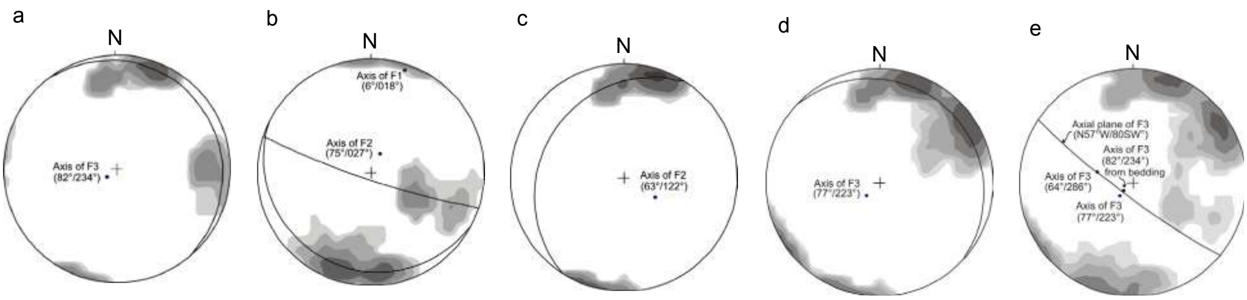

Figure 3. Stereograms of mesoscopic structural data for Wadi Road El-Sayalla metavolcanics rocks, Eastern Desert, Egypt. All stereograms are Schmidt net equal-area lower hemisphere projection. a – density contour of the poles to the bedding planes, contours at 4, 8, 16 and 32% for 32 bedding; b – density contour of the poles to the foliation from the NW and N limbs of a regional F1 and F2 isoclinal antiform, contours at 2, 4, 8 and 16% for 34 foliations; c – density contour of the poles to the foliation from the south limb of a regional F2 isoclinal antiform, contours at 3, 6, 12, 24 and 48% for 32 foliations; d – density contour of the poles to the foliation from the S and SW limbs of a regional F3 upright fold, contours at 1, 2, 4, 8 and 16% for 75 foliations; e – the great circle of best fit for F3 hinges gives an estimate of the orientation of the F3 axial plane, contours at 1, 2, 4, 8 and 16% for 109 foliations.
Рисунок 3. Стереограммы мезоскопических структурных данных для метавулканических пород из Вади-роуд Эль-Саялла, Восточная пустыня, Египет. Все стереограммы – это проекция, сохраняющая равенство площадей нижней полусферы Шмидта. а) контур плотности полюсов к плоскостям напластования, контуры 4, 8, 16 и 32% для 32 наслоений; б) контур плотности полюсов к сланцеватости из NW и N крыльев складки региональной и изоклинальной антиформы (F1 и F2), контуры 2, 4, 8 и 16 % для 34 наслоений. в) Контур плотности полюсов к сланцеватости с южного крыла складки региональной изоклинальной антиформы F2, контуры 3, 6, 12, 24 и 48 % для 32 наслоений. г) Контур плотности полюсов к сланцеватости S и SW крыльев региональной вертикальной складки F3, контуры 1, 2, 4, 8 и 16 % для 75 наслоений. д) Большой круг, наиболее подходящий для перегиба F3, дает оценку ориентации осевой плоскости F3, контуры на 1, 2, 4, 8 и 16 % для 109 наслоений.

Bedding

Bedding planes are locally preserved in the metavolcanics and measured whenever possible; they are frequently transposed by foliation and later deformation. So, the earlier ductile deformation episode can depict from the foliation. Bedding surfaces in the metavolcanics strike NW-SE and dipping generally range between 50° to 80° SW. On the lower hemisphere equal area has graphical analysis; (Fig. 3, a) indicates a great circle with fold axis plunging (82°/N-234°). This fold trend represents the third folding generation F3.

Foliation

Foliations are more extensive, parallel in finer and softer beds than in harder beds and bands of the metavolcanics especially in the more felsic metavolcanics. Foliation planes resulted from deformation which flattened the embedded clasts. One distinctive

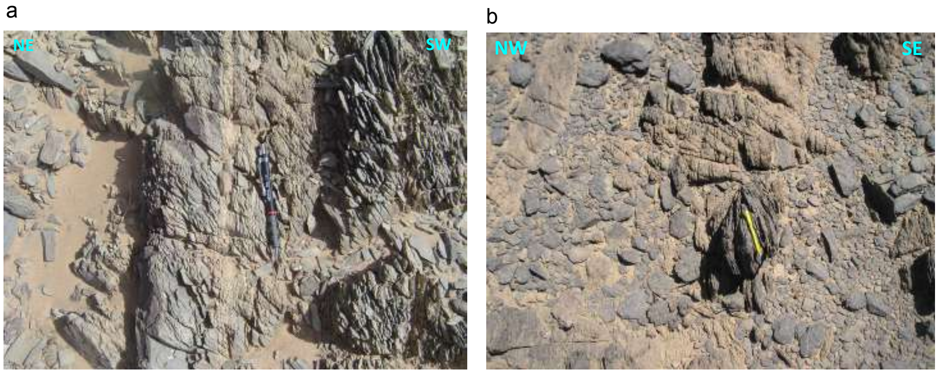

Figure 4. Effect of ductile deformation on metavolcanics. a – bedding and foliation have minor angle between each other in metavolcanics; b – banded metatuffs associating more massive basaltic shear pod.

Рисунок 4. Влияние пластической деформации на метавулканиты. а – слоистость и сланцеватость в метавулканитах разноориентированы между собой на небольшой угол; б) полосчатые метатуфы ассоциируют с разрезом более массивных базальтов.

set of cleavage is observed; it is either pervasive or penetrative and affects metavolcanics and tonalite-granodiorite along their contact. The foliations are approximately parallel to the axial surface of regional folds and are considered as an axial plane foliation representing the early folds in the area, associated with the early folding-thrusting episode [6, 11, 12]. The metavolcanics possess a strong bedding planes parallel cleavage to the foliations in some sites, have a minor angle between each other (Fig. 4, a) and others were perpendicular to the bedding planes which related to that they are located on the hinge of the fold. These bedding enclose the more massive basaltic shear pods (~30 cm long, 20 cm width) banded and ranged in thickness from (1 cm to 10 cm) (Fig. 4, b).

Folding analyses

Based on the geometric analysis of folding, three generations are distinguished F1, F2 and F3. Foliation planes are plotted on the lower hemisphere equal area projection to deduce the principal compression direction affected the metavolcanics. On the N and S limbs of F2 fold (Fig. 3, b, c), the data show bimodality of two subparallel great circles reflecting the deformation of the two limbs of an isoclinal tight fold (two limbs of F1). The elongation of pole concentrations is the result of later gentle refolding of the F1 fold limbs about F3 axial plane. The calculated F1 axis is 6°/ 018° (Fig. 3, b).

The plot of foliation poles for the N and S limbs of F2 fold; it does not show the same bimodality as the other limb due to the tightness of F1 folds on that limbs. The elongation of the polar concentration is again due to open F3 folding. The F2 axes as 75°/ 027° and 63°/ 122° (Fig. 3, b, c). The F2 fold is nearly coaxial with the F1 folds indicating that the compression during this episode (E1) continued in the same direction.

The great circle of best fit for the calculated F3 axes from bedding in metavolcanics 82°/ 234° (Fig. 3, a), and hinges of the F3 upright fold 77°/ 223° and 64°/ 286° (Fig. 3, d, e) are shown in (Fig. 3, e). This great circle defines the mean axial plane of F3 folds for the study area. Its attitude is N57°W/ 80°SW. The F3 folding is occurred by intracratonic compression episode (E2), which acted in a general NE-SW trend. The compression and shortening trend during E2 is to the NE-SW direction, i.e., quite different from the NW-SE shortening direction during E1. This means that crustal shortening directions flipped through about 90°.

The age of E1 episode can be estimated to be between the formation of the arc-inter-arc rock association and the intrusions of the syntectonic granites. These granites have an age (660–730 Ma) [13]. They are considered as emplaced at the culmination of the low angle shearing tectonic event.

The fourth folding generation F4 is manifested by syncline folding that existed in Nubian sandstone at Fileita area (Fig. 5, a, b). Bedding planes are plotted on an equal area projection to show the trend and dip of the regional fold axis F4 plunging (12°/N-83°) along the axial plane (N84°E/84°S) that existed after the intrusion of younger granites and the deposition of Nubian sandstone Post-Cretaceous.

Brittle deformation and paleostress analyses

Tectonic analyses based on the aeromagnetic survey data

Wadi Kharit/Wadi Jararah basin may be explained in terms of a pull a part wrench with right-lateral motion (Fig. 6). In pre-Jurassic time, the main trend of the basement rocks was composed mainly of NW-SE system. Tectonic analyses explain the geometric configuration and orientation of a pull a part movement which governed the sedimentation history of the area; the platform regime began in Paleozoic through northern Africa [14].

A rose diagram (Fig. 6) represents the main faults trends from an aeromagnetic map. The main trends of normal faults are NW-SE to NNW-SSE with minor trends NE-SW, E-W and N-S. On the other hand, strike slip faults have NE-SW and NNE-SSW trends. These trends can be considered as deep seated trends in the study area. From the present study; alteration processes including albitization, hematization, kaolinitization and dissilicification affecting syenogranite, alkali feldspar granite and quartz syenite are mainly associated with the NW-SE to NNW-SSE, NE-SW, E-W and N-S deep seated normal fault trends. This means that the deep seated trends from an aeromagnetic map of normal faults are the same trends of different types of alterations delineated the granitoids at Wadi Road El-Sayalla area.

Paleostress analyses

The (INVD) direct inversion [8–10, 16] used to determine paleostress tensors from fault-slip data sets. This method is based on some hypotheses which can be verified on the basis of data consistency after computations and geological observation at data collection sites: 1) The stress field was homogeneous within the site studied for the tectonic event considered. 2) Slip occurred in

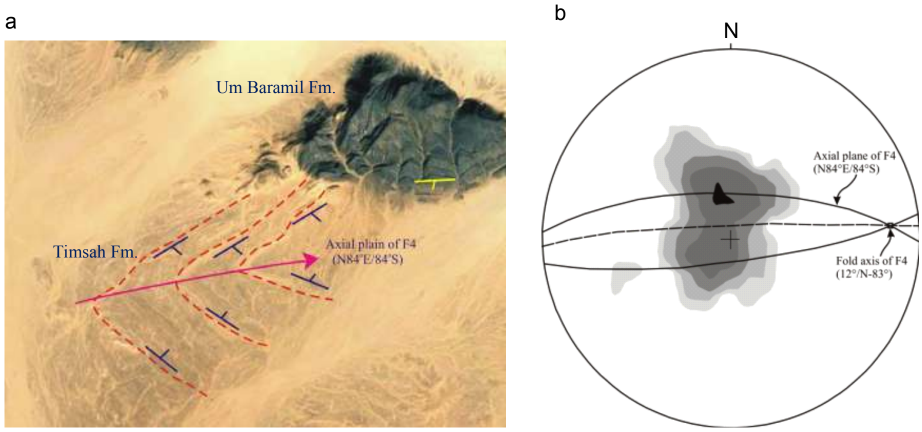

Figure 5. Folding in Nubian sandstone. a – false colored photo showing synclinal fold comprising Timsah Formation and bedding in Um Baramil Formation, photo looking to north; b – graphical solution of contoured poles to bedding associated in Nubian sandstone at Fileita area, contours at 2, 4, 8, 16 and 32% for 81 bedding.

Рисунок 5. Складчатость в нубийских песчаниках. а – цветная фотография, показывает синклинальную складку, состоящую из отложений Тимсахской свиты и слоев в Ум-Барамильской свите, объектив фотоаппарата направлен на север; b – графическое решение оконтуренных полюсов к осадочным слоям в нубийских песчаниках в районе Филейты, контуры 2, 4, 8, 16 и 32 % для 81 наслоений.

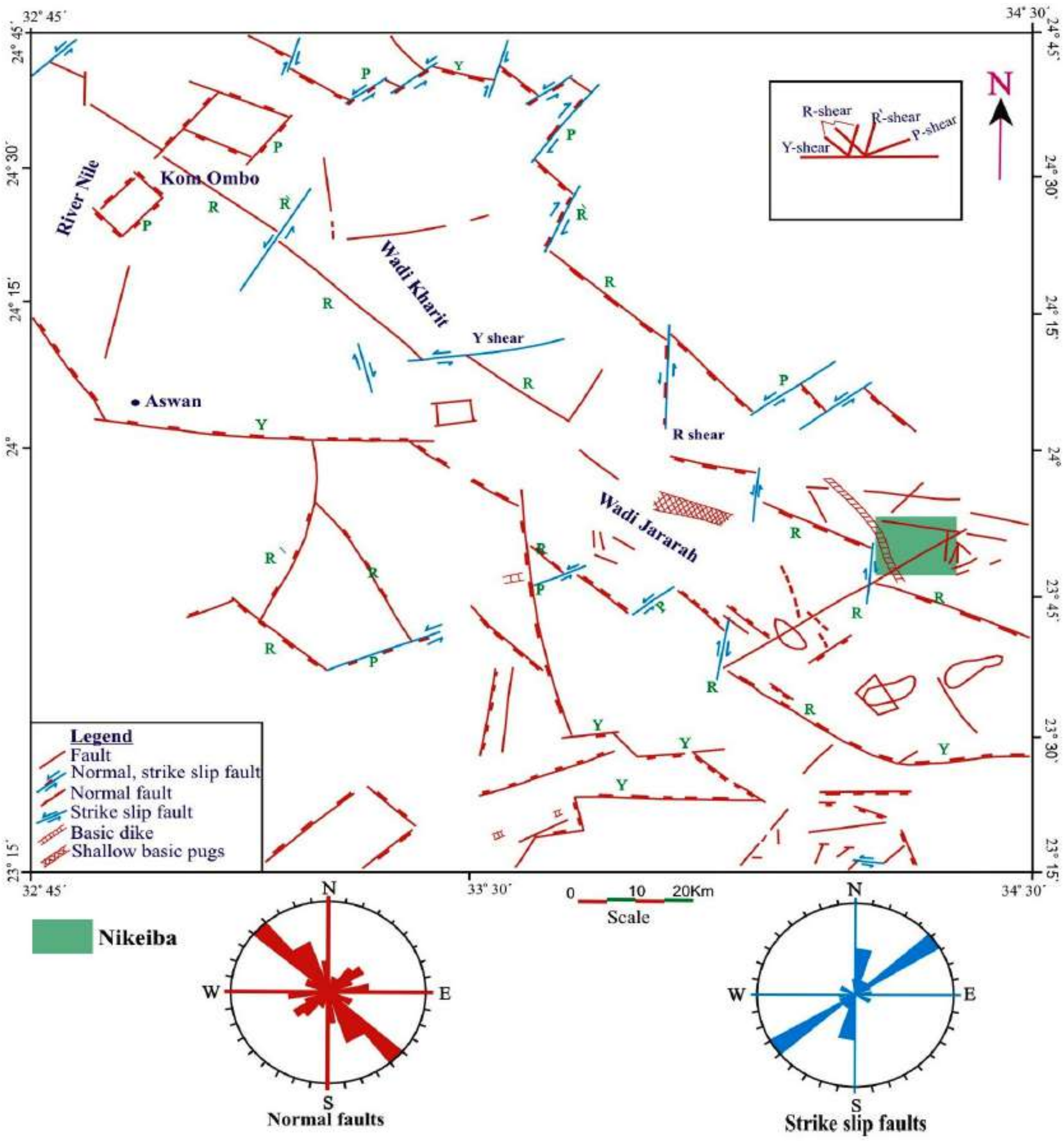

Figure 6. Interpreted tectonic map and rose diagram showing faults trends based on aeromagnetic data for Wadi Kharit / Wadi Jararah area, Eastern Desert, Egypt, after [15].

Рисунок 6. Интерпретированная тектоническая карта и роза-диаграмма, показывающие направления разломов на основе аэромагнитных данных для района Вади-Харит/Вади-Джарара, Восточная пустыня (Египет), по [15].

the direction of the maximum resolved shear stress along the fault plane and corresponds to the measured striae. 3) Faults moved independently but consistently with a single and common stress tensor during the tectonic event. 4) Fault displacement is small relative to the fault surface area [16, 17]. Paleostress reconstruction of brittle deformation is based on the analysis of fault slip data using computer programs of tensor [8–10, 16]. These methods depend on determining the best fitting reduced paleostress tensor for a given fault slip data set. The direction of slip on a fault plane depends on the orientation of the maximum (σ_1), intermediate (σ_2), and minimum (σ_3) principal stress axes and on the ratio $\Phi = (\sigma_2 - \sigma_3)/(\sigma_1 - \sigma_3)$. This ratio provides a convenient index to characterize the relationship between the principal stress magnitudes. It ranges from 0 (meaning that $\sigma_2 = \sigma_3$) to 1 (meaning that $\sigma_1 = \sigma_2$). Whereas simple extension generally corresponds to high values of Φ (e.g., > 0.5), multidirectional extension is characterized by low values that make σ_2/σ_3 stress permutation easier. In compressional tectonics, changes between reverse and strike-slip faulting modes generally correspond to situations with low values of Φ, down to about zero [18]. A quality estimator of data dispersion is the average "ratio upsilon" of RUP. Possible value of estimator RUP ranges from 0% (maximum shear stress parallel to slip with the same sense) to 200% (maximum shear stress parallel to slip with opposite sense). The average ratio of the direct inversion method (RUP) in percent (100) value < 75% = good consistency [19] as, it generally corresponds to good fits between actual fault slip data distribution and computed shear stress distribution. Another quality estimator is calculated, ANG as to the average angle (in degrees) between the measured lineation and the computed slip lineation. The results are acceptable for values between 1° to 25° [19] which are the case of the present analyses.

In the present study, paleostress tensor analyses have been conducted in the studied area based on crosscutting and geometrical relationships between faults and dikes. Twenty-one stations have been studied in which 166 fault slip data were used in calculation. Their analyses allow the calculation of 21 paleostress tensors. There are 29 faults characterizing extension, 132 faults characterizing simple shear (compressional) regime and 5 faults characterizing pure shear regime.

A - Extensional stress regime

It has been defined fault-slip data sets of system in 5 sites (Table 1) and (Fig. 7). These systems are gathered into different extensional regimes NW-SE, NNW-SSE, NE-SW and NNE-SSW. The faults recording NW-SE to NNW-SSE striking extension are found in two sites of the area (sites 104A and 109B). While the faults recording nearly NE-SW and NNE-SSW-striking extensions are recorded in three sites (111N, 3/6C and 91A). The average orientations of σ_3 axes are N-315° and N-170° for NW-SE and NNW-SSE-striking extension, N-226° and N-45° for NE-SW extension and N-196° for NNE-SSW extension. The different alteration processes encompass albitization, hematitization, kaolinitization and dissilicification affected Wadi Road El-Sayalla granitoid plutons are similar to those trends of normal deep seated faults resulted from an aeromagnetic map. These fault trends are NW-SE to NNW-SSE, NE-SW, E-W and N-S in which reveal NE-SW to ENE-WSW, NW-SE, N-S, and E-W extensional trending minimum stress (σ_3). These extensional trends considered the most important trends for higher radioactive zones at Nikeiba area as reported by [20].

B - Compressional stress regime

It has been defined using 137 faults from simple shear system and 5 faults from pure reverse compression system in 16 sites (Table 1) and (Fig. 7). These systems are gathered into five events of different compressional regimes N-S, NNW-SSE, NW-SE, E-W and NE-SW. The strike-slip regime (σ_2 vertical with horizontal σ_1 and σ_3) occurs in 15 sites. The compressional event is detected from strike-slip systems (sites 91, 3/6D for N-S while 109 and 3/6 for NNW). The computed σ_1 for this system plunges 14º, 39º, 4º and 15º in 187º, 172º, 156º and 337º directions. The NW-SE compressional event represents strike-slip phases (sites 92, 101A, 102, 104, 109A and 111). The computed σ_1 for these systems are 327°, 326°, 165°, 129°, 304° and 313° with plunges from 27°, 18°, 74°, 8°, 1° and 16°. From (Fig. 7) the alkali feldspar granite take an oval shape along the NW-SE direction as the same direction of the foliation planes in the metavolcanics in which their strike ranges between 120º to 160º. Quartz syenite affected by the N-S strike slip left lateral compression causing the displacement of their plutons (Fig. 7).

The faults recording E-W-striking compression is detected from two conjugate strike-slip fault systems (93 and 101). The orientations of σ_1 axis are 104º and 276º respectively with plunges 17° and 14°. The NE-SW compressional event (sites 109C, 3/6A and 3/6B, have orientation of σ_1 in 251°, 46° and 72° directions with plunges 21°, 4° and 2° respectively.

The pure compressional regime (σ_3 vertical with horizontal σ_1 and σ_2) is only detected in the NW-SE compression (reverse) (site 92A). The computed σ_1 for this system plunges 8º in 152º direction. This regime characterized by reverse fault causing highly sheared zone between syenogranite and quartz syenite. Also, the major synclinal folding (F4 generation), associated with Nubian sandstone basin at Fileita (Post-Cretaceous) and formed by pure compressional regime in NW-SE direction.

The geometry of fault populations is complex and varies from site to site. Oblique faulting is common where slip movements were initiated along pre-existing fault planes. For instance, some E-W and NW-SE trending oblique-slip faults have been reactivated into strike-slip sinstral faults (sites 102 and 92). This indicates that this event is younger than the N-S and NW-SE extensional events**.** Also, E-W trending oblique-slip faults have been reactivated into strike- slip dextral faults (sites 109C). This indicates that this event is younger than the N-S extensional event**.**

The ratio of stress differences Φ has very high value (0.5) in sites 92, 102, 104 and 111 i.e. σ_2 is very close to σ_1 so, changing between dip-slip faulting and strike-slip faulting modes can took place [18]. Conversely, where the tectonic regime is dominated by extension, a decrease in the ratio Φ results in more irregular trajectories of σ_3 and local permutations of σ_2/σ_3 [18] (site 104A and 109B).

Tectonic evolution of Road El-Sayalla area

The following geological and tectonic episodes were inferred from the present study and the geochronological data for the surrounding areas were published (Fig. 8).

Syen-tectonic granite; folding-thrusting episode (E1)

It was associated with the cratonization of the arc-inter-arc rock association. Low angle thrusting, tight and isoclinal folds of (F1) were formed during this stage (E1). Sol Hamed-Onib and Allaqi-Heiani sutures were formed due to the collision between Gerf and Gabgaba-Gebeit terrains (> 715 Ma [13]. Also, the metavolcanics are similar expressions of the ~ 750 Ma crust-forming events [21]. The compression during early folding-thrusting episode (E1) continued in the same direction to generate nearly coaxial folds (F2) with (F1). The F2 folds were formed between formation of arc-inter-arc rock association and the intrusion of the syntectonic granites 660–730 Ma [13]. The intrusion of these granites represent the end of folding-thrusting episode (E1).

Results of paleostress tensor from the measured fault-slip data at Wadi Road El-Sayalla area, Eastern Desert, Egypt.
Результаты тензора палеостресса после измерения данных о разломах в Вади-роуд Эль-Саялла, Восточная пустыня (Египет).

Site No.	Tensor	Axe σ_1		Axe σ_2		Axe σ_3		Φ	ANG	RUP	Conj. No.
		D	*P*	*D*	*P*	*D*	*P*				
91A	Ex	20°	78°	287°	1°	196°	12°	0.424	3°	23	9
104A	Ex	121°	72°	224°	4°	315°	17°	0.247	3°	15	6
109B	Ex	313°	75°	78°	9°	170°	12°	0.249	2°	10	4
3/6C	Ex	188°	82°	315°	5°	45°	6°	0.390	2°	10	5
111N	Ex	29°	71°	134°	5°	226°	18°	0.33	6°	21	5
3/6D	Cp2	172°	39°	285°	26°	39°	40°	0.402	4°	48	8
91	Cp2	187°	14°	54°	69°	280°	14°	0.506	12°	34	16
92	Cp2	327°	27°	185°	56°	66°	18°	0.675	1°	12	6
93	Cp2	104°	17°	329°	67	199°	16°	0.178	3°	20	10
101	Cp2	276°	14°	33°	60	179°	26°	0.416	25°	54	16
101A	Cp2	326°	18°	137°	72°	235°	3°	0.363	9°	36	5
102	Cp2	293°	1°	202°	48°	23°	42°	0.644	4°	27	5
104	Cp2	129°	8°	348°	80°	220°	6°	0.552	4°	38	6
109	Cp2	156°	4°	50°	77°	246°	13°	0.244	11°	36	12
109A	Cp2	304°	1°	37°	70°	213°	20°	0.471	23°	49	9
109C	Cp2	251°	21°	114°	62°	348°	18°	0.176	4°	33	7
111	Cp2	313°	16°	145°	74°	44°	3°	0.524	7°	44	5
3/6	Cp2	341°	22°	162°	68°	71°	0°	0.416	7°	36	9
3/6A	Cp2	46°	4°	147°	69°	315°	21°	0.148	6°	28	12
3/6B	Cp2	72°	2°	339°	49°	163°	41°	0.256	1°	18	6
92A	Cp1	152°	8°	243°	6°	8°	80°	0.422	5°	21	5

Symbols: Ex (Extensional system), Cp2 (strike-slip shear system), Cp1 (pure compression reverse system), σ_1, σ_2 and σ_3 = principal stress axes, D = trend of axis, P = plunge of axis, $\Phi = (\sigma_2 - \sigma_3)/(\sigma_1 - \sigma_3)$. ANG = angle between calculated and measured shear. RUP = ratio upsilon (in %) of the function defined by [9] from 0% to 200% and Conj. No. = number of conjugate fault systems (total = 166).

Late-tectonic granite; upright folding episode (E2)

It was associated with compression and shortening to the NE-SW direction which different from the NW-SE shortening direction during (E1). At the end of the E2 numerous plutons of the late-tectonic granites in the Eastern Desert are intruded parallel to the NNW-SSE to NW-SE trend [22]. The folding and foliation during the E1 and E2 provided most of the space for the granitic plutons intrusion [23].

Post-tectonic granitic episode (E3)

The syenogranite and alkali feldspar granite of Nikeiba exhibit A-type affinity intruded during this episode. On the basis of petrological and geochemical data, this batch displays anorogenic features of post orogenic environment [20, 24] (E3). So, this batch of Nikeiba post-tectonic granites can be occurred during a prolonged heating event by post-collision extension [25, 26]. It is consistent with the concept that represents a continuation of magmatism in a post-orogenic environment, which reactivates major structures.

Early Cretaceous to Post Pleistocene episode (E4 and E5)

The fourth episode (E4) is manifested by syncline folding along the axial plane bedding of F4 (N84°E/84°S) that existed after the intrusion of younger granites which were detected in the Nubian sandstone at Fileita area.

Fracturing, faulting episode (E5) is manifested in the studied area by successive events of compressional reverse, strike slip faulting and extensional normal faulting. They are detected in syenogranite, alkali feldspar granite and quartz syenite. The area is dissected by multi-trends of fault populations arranged according to relative chronology starting from the oldest event: E-W strike slip (right), N-S strike slip (left), E-W dip slip, NE-SW strike slip (right) and NE-SW dip slip main trend clusters. The N-S reactivated left lateral strike-slip faults which cross cut clayey sandstone at Fileita.

Discussions and conclusion

1 – The detailed structural study reveals four tectonic episodes that affected the studied area; E1: Folding-thrusting episode; It is represented by tight and isoclinal folds (F1) associated with metavolcanics association. The compression during early folding-thrusting episode continued in the same direction to generate nearly coaxial folds (F2) with the isoclinal folds (F1). The intrusion of syntectonic granites (tonalite-granodiorite) marks the end of this episode 660–730 Ma [13].

2 – E2: Upright folding episode; It is associated with compression and shortening in the NE-SW direction, which is different from the NW-SE shortening direction during E1.

3 – E3: Post tectonic granitic intrusion episode; the syenogranite and alkali feldspar granite of Nikeiba exhibiting A-type affinity and post orogenic environment formed during a prolonged heating event by post-collision extension.

4 – E4 and E5: Early Cretaceous to Post Pleistocene episode; syncline fold, fracturing and faulting episode show the analysis of paleostress and relative chronological data indicate that the area experienced successive events of compressional and extensional regimes starting with the oldest event; E-W strike slip (right), N-S strike slip (left), E-W dip slip, NE-SW strike slip (right) and NE-SW dip slip (main trend). Trends of the main tensions occurred along the inherited axial planes of F1, F2, F3 and F4 folds in sites (104A, 109B, (111N, 3/6C) and 91A, respectively.

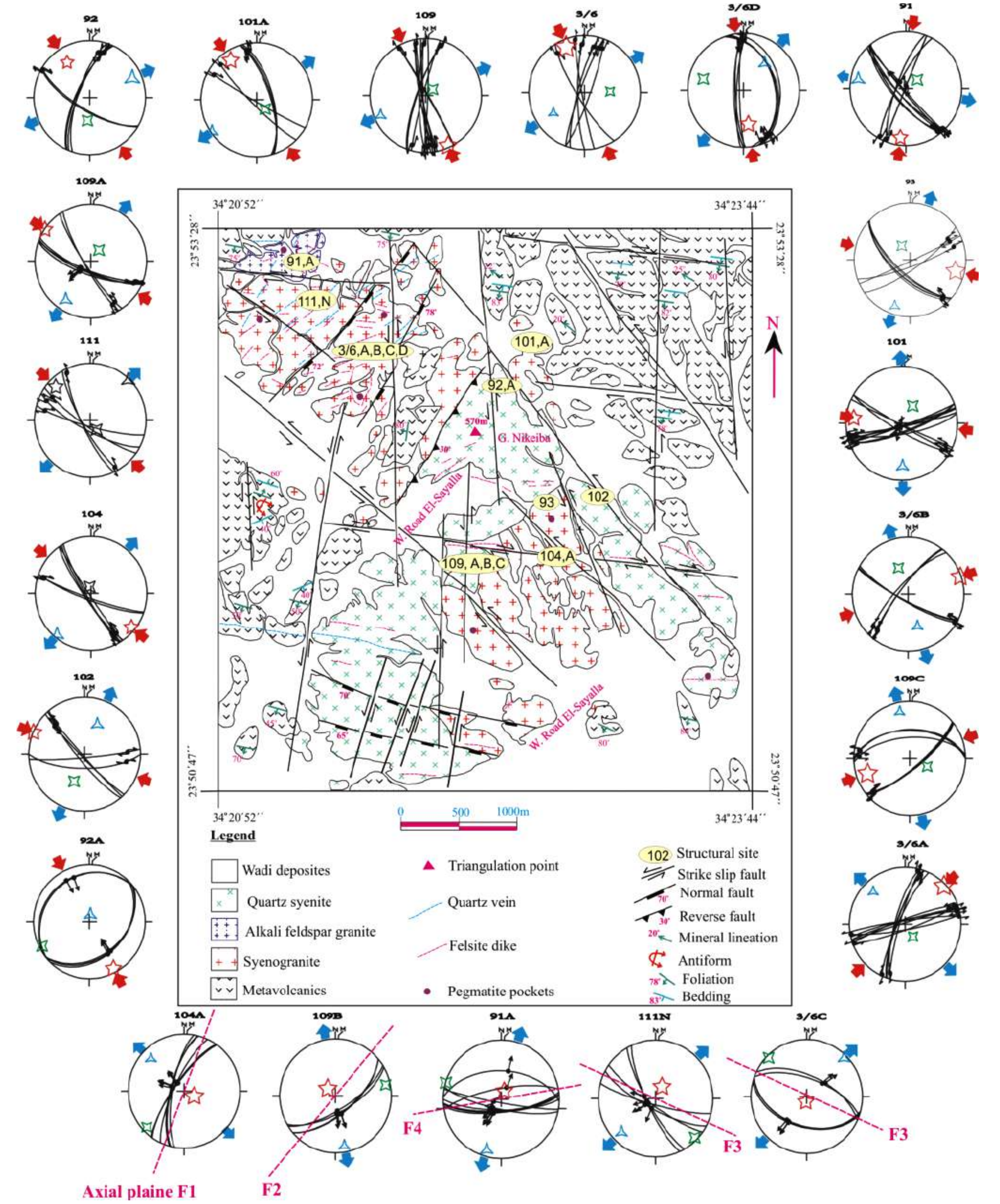

Figure 7. Lower-hemisphere Schmidt projection of fault slips data corresponding tensor for compressional and extensional phases showing their distributions on the geological map for Nikeiba plutons at Wadi Road El-Sayalla, Eastern Desert Egypt. *Symbols*: as 5-pointer star (red color) = σ_1, 4-pointer star (green color) = σ_2, 3-pointer star (blue color) = σ_3; Large blue and red arrows = direction of extension and compression, small arrows indicate slickenside sense of movement.

Рисунок 7. Нижняя полусфера проекции Шмидта данных истинной высоты сброса; соответствует тензору для растянутых и сжатых фаз, показывающих их распределение на геологической карте, для плутонов Никейба на Вади-роуд Эль-Саялла, Восточная пустыня (Египет). *Обозначения:* в виде звезды с 5 наконечниками (красный цвет) = σ_1, звезда с 4 наконечниками (зеленый цвет) = σ_2, звезда с тремя наконечниками (синий цвет) = σ_3; Большие синие и красные стрелки = направление растяжения и сжатия, маленькие стрелки указывают на зеркало скольжения.

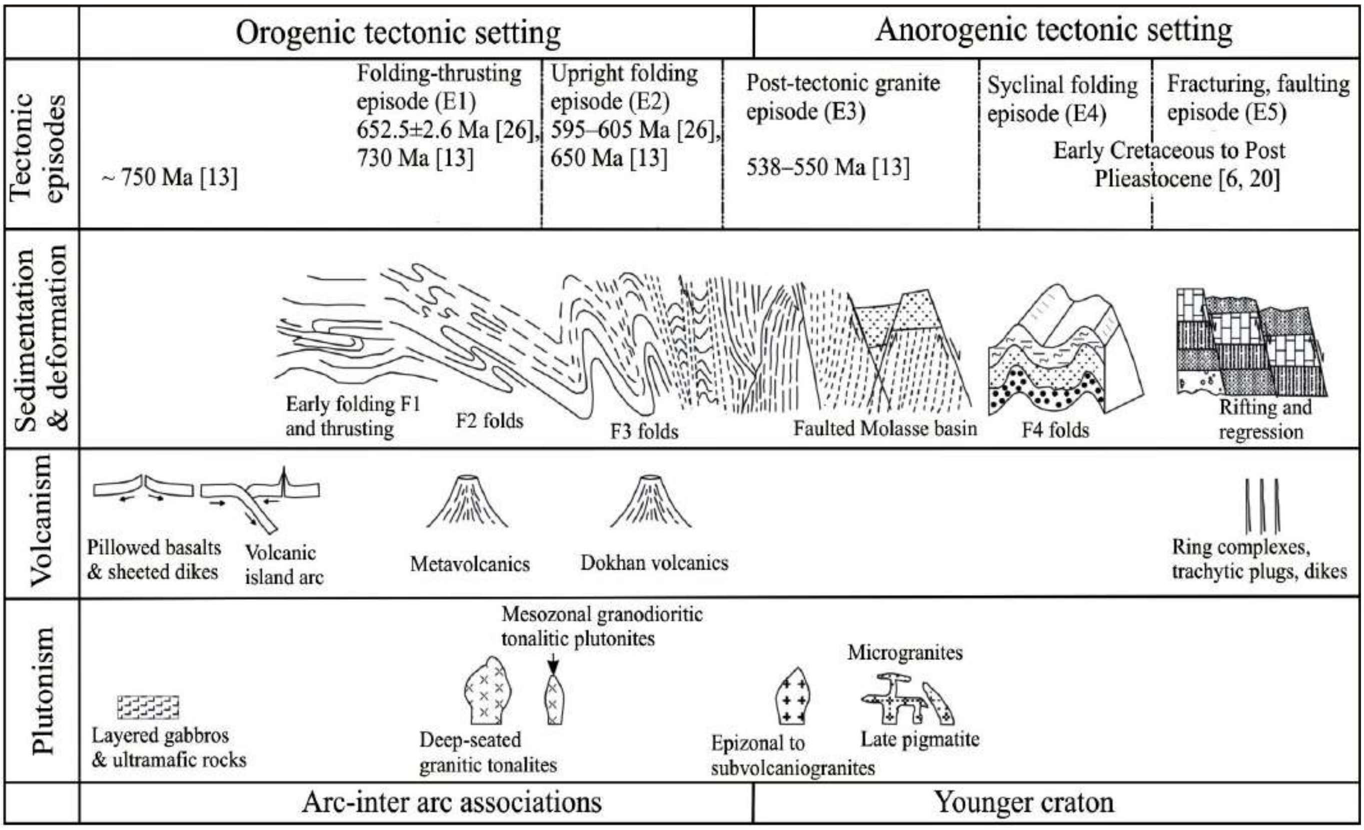

Figure 8. Tectono-stratigraphic sequence of rock association of the basement complex and non-conformable Nubian sandstone at Wadi Road El-Sayalla in the Eastern Desert, Egypt, modified after [6].
Рисунок 8. Тектоно-стратиграфическая последовательность ассоциирующих пород из комплексов основания и несогласие нубийского песчаника в Вади-роуд Эль-Саялла в Восточной пустыне, Египет, с изменениями по [6].

5 – The NW-SE, NE-SW, E-W, NNW-SSE and N-S normal fault trends control multi injections and many alteration features. They are considered as important trends for deep seated structures from aeromagnetic map and could have acted as good directions for the radioactive mineral (thorite and uranothorite).

6 – Mineralization appears to be structurally controlled by the interaction between inherited ductile fabrics and overprinting brittle structures. During reactivation, simple shear parallel to the inherited ductile fabrics was responsible for development of mineralized structures. Also, uranium and thorium are concentrated in accessory minerals, especially uranothorite, monazite, zircon, allanite yttrocolombite and fluorite in which they are associated with the highly altered syenogranite, alkali feldspar, quartz syenite, felsite dikes and pegmatite pockets in Nikeiba plutons at Wadi Road El-Sayalla.

REFERENCES

1. Ghebreab W. 1998, Tectonics of the Red Sea region reassessed. *Earth-Science Reviews*, vol. 45, issues 1–2, pp. 1–44. https://doi.org/10.1016/S0012-8252(98)00036-1
2. Abdelsalam M. G., Abdeen M. M., Dowidar H. M., Stern R. J., Abdelghaffar A. A. 2003, Structural evolution of the Neoproterozoic western Allaqi-Heiani suture zone, Southern Egypt. *Precambrian Research*, vol. 124, issue 1, pp. 87–104. https://doi.org/10.1016/S0301-9268(03)00080-9
3. Helmy H. M., Kaindl R., Fritz H., Loizenbauer J. 2004, The Sukari gold mine, Eastern Desert, Egypt: structural setting, mineralogy and fluid inclusion study. *Mineralium Deposita*, vol. 39, pp. 495–511. https://doi.org/10.1007/s00126-004-0426-z
4. Abdeen M. M., Greiling R. O. 2005, A quantitative structural study of late Pan-African compressional deformation in the central Eastern Desert (Egypt) during Gondwana assembly. *Gondwana Research*, vol. 8, issue 4, pp. 457–471. https://doi.org/10.1016/S1342-937X(05)71148-5
5. Zoheir B. A. 2008, Structural controls, temperature–pressure conditions and fluid evolution of orogenic gold mineralization in Egypt: a case study from the Betam gold mine, south Eastern Desert. *Mineralium Deposita*, vol. 43, issue 1, pp. 79–95. https://doi.org/10.1007/s00126-007-0156-0
6. Ali K. G. 2011, Structural control of El Sela granites and associated uranium deposits, south Eastern Desert, Egypt. *Arabian Journal of Geosciences*, vol. 6, issue 6, pp. 1753–1767. https://doi.org/10.1007/s12517-011-0489-y
7. Ibrahim W. S., Watanabe K., Ibrahim M. E., Yonezu K. 2015, Neoproterozoic Tectonic Evolution of Gabal Abu Houdied Area, South Eastern Desert, Egypt: As a Part of Arabian–Nubian Shield Tectonics. *Arabian Journal for Science and Engineering*, vol. 40, issue 7, pp. 1947–1966. https://doi.org/10.1007/s13369-014-1521-9
8. Angelier J. 1989, From orientation to magnitudes in paleostress determinations using fault slip data. *Journal of Structural Geology*, vol. 11, pp. 37–50. https://doi.org/10.1016/0191-8141(89)90034-5
9. Angelier J. 1990, Inversion of field data in fault tectonics to obtain the regional stress-III. A new rapid direct inversion method by analytical means. *Geophysical Journal International*, vol. 103, issue 2, pp. 363–376. https://doi.org/10.1111/j.1365-246X.1990.tb01777.x
10. Angelier J. 1994, Fault slip analysis and paleostress reconstruction. *In: Hancock P. L. (ed.), Continental deformation*. Oxford, New York, Seoul, Tokyo: Pergamon Press, pp. 53–100. ISBN 978-0080379302; 0080379311.
11. Abdel Meguid A. A. 1986, Geologic and radiometric studies of uraniferous granites in Um Ara-Um Shilman area south Eastern Desert, Egypt. PhD thesis, Suez Canal University, Egypt. 222 p.
12. Ali K. G., Gaafar I. M., Ibrahim T. M. 2008, Structural control and geophysical signature of Kab Amiri Epi syenitized muscovite granite and associated uranium showings, central Eastern Desert, Egypt. *Annals of the Geological Survey of Egypt*, vol. XXX, pp. 21–41.

13. Stern R. J., Kroner A., Manton W. I., Reischmann T., Mansour M., Hussein I. M. 1989, Geochronology of the late Precambrian Hamisana shear zone, Red Sea Hills, Sudan and Egypt. *Journal of the Geological Society*, vol. 146, issue 6, pp. 1017–1029. https://doi.org/10.1144/gsjgs.146.6.1017
14. Meshref W. M. 1990, Tectonic framework. *In: R. Said (ed.), The Geology of Egypt.* Rotterdam, Brookfield: A. A. Balkema, pp. 113–155. ISBN 90-6191-856-1.
15. Hanafy S. M. 1997, Geological, aeromagnetic and aeroradiometric studies of Wadi Jararah area, South Eastern Desert, Egypt. M. Sc. thesis, Faculty of science, Cairo University, 104 p.
16. Angelier J. 1984, Tectonic analysis of fault slip data sets. *Journal of Geophysical Research. Solid Earth*, vol. 89, issue 87, pp. 5835–5848. https://doi.org/10.1029/JB089iB07p05835
17. Faure S., Tremblay A., Angelier J. 1996, State of intra-plate stress and tectonism of northeastern America since Cretaceous times, with particular emphasis on the New England-Quebec igneous province. *Tectonophysics*, vol. 255, issues 1–2, pp. 111–134. https://doi.org/10.1016/0040-1951(95)00113-1
18. Hu J. C., Angelier J. 2004, Stress permutations: Three-dimensional distinct element analysis accounts for a common phenomenon in brittle tectonics. *Journal of Geophysical Research. Solid Earth*, vol. 109, issue B9, B09403. https://doi.org/10.1029/2003JB002616
19. Bergerat F., Angelier J. 1998, Fault systems and paleostresses in the Vestfirdir Peninsula. Relationships with the Tertiary paleo-rifts of Skagi and Snaefells (Northwest Iceland). *Geodinamica Acta*, vol. 11, issue 2–3, pp. 105–118. https://doi.org/10.1080/09853111.1998.11105313
20. Abdel Gawad A. E. 2011, Geology and radioelements potentialities of unconformable basement-sedimentary rocks at G. Nikeiba and G. Fileita areas, south Eastern Desert, Egypt. PhD thesis, Faculty of Science, Minufiya University, Egypt, 141 p.
21. Ali K. A., Stern R. J., Manton W. I., Kimura J. I., Khamees H. A. 2009, Geochemistry, Nd isotopes and U–Pb SHRIMP zircon dating of Neoproterozoic volcanic rocks from the central Eastern Desert of Egypt: New insights into the ~750 Ma crust-forming event. *Precambrian Research*, vol. 171, issues 1–4, pp. 1–22. https://doi.org/10.1016/j.precamres.2009.03.002
22. Abdel Meguid A. A. 1992, Late Proterozoic Pan-African tectonic evolution of the Egyptian part of the Arabian-Nubian Shield. Middle East Research Center (M. E. R. C.) Ain Shams University, Earth Sc. Ser., vol. 6, pp. 13–28.
23. Cobbing J. 2000, The geology and mapping of granite batholiths. Springer, Berlin, Heidelberg, 141 p. ISBN 978-3-540-67684-3. https://doi.org/10.1007/3-540-45055-6
24. Eliwa H. A., Ali K. G., Masoud S. M., Murata M., Abdel Gawad A. E. 2018, Geochemical features of granitoids at Nikeiba area, Eastern Desert, Egypt // *Vserossiyskaya nauchnaya konferentsiya “Ural'skaya mineralogicheskaya shkola-2018”* [XXIV All-Russian scientific conference “Ural Mineralogical School-2018”]. 280 p. URL: http://www.igg.uran.ru/sites/default/files/Conferences/minshkola-2018_abstracts.pdf
25. Xie Z., Zheng Y. F., Zhao Z. F., Wu Y. B., Wang Z., Chen J., Liu X., Wu F. Y. 2006, Mineral isotope evidence for the contemporaneous process of Mesozoic granite emplacement and gneiss metamorphism in the Dabie orogen. *Chemical Geology*, vol. 231, issue 3, pp. 214–235. https://doi.org/10.1016/j.chemgeo.2006.01.028
26. Moussa E. M. M., Stern R. J., Mantonb W. I., Ali K. A. 2008, SHRIMP zircon dating and Sm/Nd isotopic investigations of Neoproterozoic granitoids, Eastern Desert, Egypt. *Precambrian Research*, vol. 160, issues 3–4, pp. 341–356. https://doi.org/10.1016/j.precamres.2007.08.006

The article was received on September 10, 2018

УДК 551.243(620) https://doi.org/10.21440/2307-2091-2018-4-7-17

Структурная эволюция района Вади роуд Эль-Саялла, Восточная пустыня (Египет)

Халед Гамаль АЛИ[1],
Хасан Али ЭЛИВА[2],
Масуд Салах МАСУД[1],
Мамору МУРАТА[3],
Ахмед Эль Саед АБДЕЛЬ ГАВАД[1,*],

[1]Управление ядерных материалов, Каир, Египет
[2]Университет Минуфия, Каир, Египет
[3]Университет Наруто, National University Corporation, Наруто, Япония

Район Вади роуд Эль-Саялла является частью юга Восточной пустыни Египта. Он состоит из двух плутонов, основания комплексов горных пород Никейба и песчаников Филейта Нубиан. В состав плутонов Никейба входят метавулканиты, сиенограниты, щелочные полевошпатовые граниты и кварцевые сиениты, прорванные дайками фельзитов и долеритов и кварцевыми жилами, все эти комплексы пород несогласно перекрываются нубийскими песчаниками в районе Филейты.

Цель работы. Исследование заключается в выяснении взаимодействия между унаследованными пластическими структурно-текстурными элементами и наложением хрупких структур. Важно реконструировать тектоническую эволюцию района Вади-роуд Эль-Саялла, что поможет определить границы минерализации в исследуемой области.

Методы исследования. Анализировалось сгибание, связанное с пластическими структурно-текстурными элементами, с использованием программных пакетов стереографической проекции GE Orient версии 9.4.5. Анализ трещин, связанных с хрупкими структурами, проводился количественно с использованием палеостресс анализов различных наборов для расчета тензоров, связанных с различными событиями сжатия и экстенсионализации с использованием программы Tensor.

Результаты. Структурная эволюция в исследуемой области подразделяется на пять структурных эпизодов: E1: синтектонический гранит (тоналит-гранодиорит); эпизод сгибания, связанный с кратонизацией островодужных и междуговых комплексов пород. E2: позднетектонический гранит; эпизод прямой складки, связанный со сжатием в направлении NE-SW. E3: Интрузии посттектонических гранитов с образованием сиеногранитов и щелочно-полевошпатовых гранитов Никейбы. E4 и E5: от раннемелового до постплейстоценского периодов проявляется синклинальное сгибание вдоль направления ENE-WSW в нубийском песчанике Филейта (E4). С другой стороны, E5: Разрушение, тектоническая зона характеризуется многочисленными разломами (сдвиговый разлом EW (правый, самый старый), сдвиговый разлом NS (левый), вертикальное смещение E-W, сдвиговый разлом NE-SW (правый) и NE-SW вертикальное смещение (самое молодое). Акцессорные минералы, такие как торит, уранторит, монацит, циркон, аланит, иттроколумбит и флюорит, по-видимому, структурно контролируются взаимодействием между унаследованными пластическими структурно-текстурными элементами и наложением хрупких структур. Нормальные сбросы NE-SW, NW-SE, E-W, NNW-SSE и N-S являются важными глубоко залегающими структурами, которые контролируют многочисленные дайки фельзитов и долеритов и соответственно наложенные изменения, которые могут нести различную рудную минерализацию.

Ключевые слова: Вади роуд Эль-Саялла, Никейба, Филейта, Египет, сдвиговая складчатость, кратонизация, образование складчатости, образование разломов.

Статья поступила в редакцию 10 сентября 2018 г.

* gawadnma@gmail.com
http://orcid.org/0000-0002-2014-2677